






ORIGINAL RESEARCH

Effects of High Fat Versus Normal Diet on Extracellular Vesicle–Induced Angiogenesis in a Swine Model of Chronic Myocardial Ischemia

Ahmed Aboulgheit, MD; Brittany A. Potz, MD; Laura A. Scrimgeour, MD; Catherine Karbasiafshar , BS; Guangbin Shi, MD; Zhiqi Zhang, MD; Jason T. Machan , PhD; Christoph Schorl, PhD; Alexander S. Brodsky, PhD; Karla Braga , MS; Melissa Pfeiffer , MS; May Gao; Olivia Cummings; Neel R. Sodha, MD; M. Ruhul Abid , MD, PhD; Frank W. Sellke, MD

BACKGROUND: Mesenchymal stem cell–derived extracellular vesicles (EVs) promote angiogenesis in the ischemic myocardium. This study examines the difference in vascular density, myocardial perfusion, molecular signaling, and gene expression between normal diet (ND) and high fat diet (HFD) groups at baseline and following intramyocardial injection of EVs.

METHODS AND RESULTS: Intact male Yorkshire swine fed either an ND (n=17) or HFD (n=14) underwent placement of an ameroid constrictor on the left circumflex coronary artery. Subsequently, animals received either intramyocardial injection of vehicle-saline as controls; (ND-controls n=7, HFD-controls, n=6) or EVs; (ND-EVs n=10, HFD-EVs n=8) into the ischemic territory. Five weeks later, myocardial function, perfusion, vascular density, cell signaling, and gene expression were examined. EVs improved indices of myocardial contractile function, myocardial perfusion, and arteriogenesis in both dietary cohorts. Interestingly, quantification of alpha smooth muscle actin demonstrated higher basal arteriolar density in HFD swine compared with their ND counterparts; whereas EVs were associated with increased CD31-labeled endothelial cell density only in the ND tissue, which approached significance. Levels of total endothelial nitric oxide synthase, FOXO1 (forkhead box protein O1), transforming growth factor- β , phosphorylated VEGFR2 (vascular endothelial growth factor receptor 2), and phosphorylated MAPK ERK1/ERK2 (mitogen-activated protein kinase) were higher in ischemic myocardial lysates from ND-controls compared with HFD-controls. Conversely, HFD-control tissue showed increased expression of phosphorylated endothelial nitric oxide synthase, phosphorylated FOXO1, VEGFR2, and MAPK ERK1/ERK2 with respect to ND-controls. Preliminary gene expression studies indicate differential modulation of transcriptional activity by EVs between the 2 dietary cohorts.

CONCLUSIONS: HFD produces a profound metabolic disorder that dysregulates the molecular mechanisms of collateral vessel formation in the ischemic myocardium, which may hinder the therapeutic angiogenic effects of EVs.

Key Words: angiogenesis ■ chronic myocardial ischemia ■ extracellular vesicles ■ high fat diet ■ hyperglycemia ■ stem cells

Myocardial ischemia accounts for the leading cause of death worldwide.¹ Currently, therapeutic options include pharmacological therapy² and revascularization where clinically warranted, either by percutaneous coronary intervention³ or surgical

bypass grafting.⁴ In patients who are not candidates for traditional methods of revascularization, regenerative therapies have been studied. Despite many preclinical laboratory data that demonstrate robust improvement in myocardial function and perfusion, to

Correspondence to: Frank W. Sellke, MD, Alpert Medical School, Brown University, 2 Dudley Street, MOC 360, Providence, RI 02905. E-mail: fsellke@lifespan.org

Supplementary Material for this article is available at <https://www.ahajournals.org/doi/suppl/10.1161/JAHA.120.017437>.

For Sources of Funding and Disclosures, see page 15.

© 2021 The Authors. Published on behalf of the American Heart Association, Inc., by Wiley. This is an open access article under the terms of the Creative Commons Attribution-NonCommercial-NoDerivs License, which permits use and distribution in any medium, provided the original work is properly cited, the use is non-commercial and no modifications or adaptations are made.

JAHA is available at: www.ahajournals.org/journal/jaha

CLINICAL PERSPECTIVE

What Is New?

- Many novel translational therapies are successful in animal models but have limited application in clinical practice because of complex disease involving highly prevalent comorbidities such as diabetes mellitus and hypertension.
- Mesenchymal stem cell–derived extracellular vesicles are an exciting therapeutic modality with promising results in our swine model of chronic myocardial ischemia. Interestingly, we found that the proangiogenic effects of extracellular vesicles were inhibited with administration of a high fat diet.
- This study identifies a number of key aberrancies in molecular signaling and gene expression that are associated with dyslipidemia and impaired glucose tolerance.

What Are the Clinical Implications?

- Elucidating the molecular basis of the maladaptive changes that occur in the ischemic myocardium with metabolic stress may provide critical insight that guides prospective therapeutic strategies.
- In this context, we propose that extracellular vesicles are complex, versatile signaling vehicles that can potentially be modified to incorporate corrective signals targeted to specific erroneous molecular events.
- This would allow for potentiation of the therapeutic effects of extracellular vesicles and other novel treatments, thus offering sustainable outcomes in clinical practice.

Nonstandard Abbreviations and Acronyms

αSMA, ALLSTAR	alpha smooth muscle actin Allogeneic Heart Stem Cells to Achieve Myocardial Regeneration
Akt	protein kinase B
BAX	BCL2-associated apoptosis regulator
dp/dt	derivative of pressure over time
eNOS	endothelial nitric oxide synthase
EV	extracellular vesicle
FDR	false discovery rate
FOXO1	forkhead box protein O1
GEO	Gene Expression Omnibus

HFD	high fat diet
HFDC	high fat diet control
HFD-EV	high fat diet extracellular vesicle
LCx	left circumflex coronary artery
MMP-9	matrix metalloproteinase 9
MAPK ERK1/ERK2	mitogen-activated protein kinase
ND	normal diet
NDC	normal diet control
ND-EV	normal diet extracellular vesicle
TGF-β	transforming growth factor-β
Tau	left ventricular diastolic time constant
VEGFR2	vascular endothelial growth factor receptor 2

date, translational applications have largely failed to improve clinical outcomes or even provide symptomatic relief. The disparity between results in laboratory animals and clinical trials may lie in the inhibitory effects of biological factors, such as hyperglycemia⁵ and hypercholesterolemia.⁶

Stem cell therapy has been extensively studied in the context of refractory coronary artery disease and heart failure. Indeed, the notion that a multipotent dividing cell population with regenerative capacity may give rise to myocardial cell lines in a structured manner, which thereby promotes formation of a vascular network capable of sustaining viability to the nascent tissue, holds promise. However, it is now generally considered that stem cell therapy produces a trophic effect rather than providing the cellular substrate for vascular or myocardial regeneration. The ALLSTAR (Allogeneic Heart Stem Cells to Achieve Myocardial Regeneration) trial, among other stem cell–based clinical trials, demonstrated short-lived effects of treatment with intracoronary allogeneic stem cells, lacking the sustainability that would permit consideration of their use in a clinical setting.⁷ Despite the autologous nature of mesenchymal stem cells used in such studies, immunological-mediated inhibition of homing and progression of the implanted cells into functional cardiac elements may have contributed to their rapidly subsiding actions.⁸

Mesenchymal-derived stem cells and other progenitor cells secrete active bioproducts; extracellular vesicles (EVs) mediate the many actions of stem cells through a wide range of paracrine signaling mechanisms with subsequent modulation of target

cell proliferation, immunogenicity, and response to injury. These organelles represent a higher order signaling mechanism; their double-layered lipid coat envelops many molecular moieties such as small interfering RNA (siRNA), cytokines, growth factors, and other proteins that target pathways in a coordinated manner.⁹

Previously, our group has demonstrated the efficacy of EV therapy in promoting angiogenesis and collateral-dependent myocardial perfusion in our validated swine model of chronic myocardial ischemia.^{10,11} This study demonstrates that the high fat diet (HFD) model produced hyperglycemia and hypercholesterolemia among other characteristics of type 2 diabetes mellitus or metabolic syndrome.^{10–12} Furthermore, many remarkable differences were observed in response to EV therapy between HFD and normal diet (ND) animals, with emphasis on the molecular basis and differential gene expression contributing to an aberrant regenerative capacity.

METHODS

Swine Model of Chronic Myocardial Ischemia: Dietary Effects

All animal care and procedures were conducted alongside veterinary staff, in accordance with protocols approved by the Institutional Animal Care and Use Committee of Rhode Island Hospital (Lifespan). The data, analytic methods, and study materials are and will continue to be made available to other parties, on request, for the purpose of reproducibility. Thirty-one intact male Yorkshire swine were fed either an ND (n=17) or a daily 500-g/d HFD (n=14) consisting of 4% cholesterol, 17.2% coconut oil, 2.3% corn oil, 1.5% sodium cholate, and 75% regular chow (Sinclair Research). This diet is a validated method of producing clinically relevant characteristics of metabolic syndrome in swine such as hypertension, dyslipidemia, and impaired glucose tolerance.¹²

Surgical Procedure

At 11 weeks of age, animals underwent the initial procedure, which included placement of an ameroid constrictor on the left circumflex coronary artery (LCx).^{10,11} Following preoperative antibiotic prophylaxis and antiplatelet therapy, general anesthesia was induced with intramuscular Telazol (4.4 mg/kg) and Xylazine (2.2 mg/kg). The chest was entered via a left thoracotomy and the LCx was identified and dissected in the left atrioventricular groove. A vessel loop was placed around the artery and was used to occlude it for a duration of 2 minutes (which produced ST elevation on ECG tracings consistent with

ischemia in the target territory). After LCx occlusion, 5 mL of gold microspheres (BioPal) were injected into the left atrial appendage. Next, an ameroid constrictor (Research Instruments SW) of appropriate size was selected by the surgical team and placed around the LCx.¹³ To prevent spasm, 1 mL of nitroglycerin solution (Baxter International) was administered topically to the LCx, and amiodarone (5 mg/kg) was given intravenously as needed to prevent arrhythmias.

Isolation of EVs

Human bone marrow–derived mesenchymal stem cells (Lonza PT-2501) were initially incubated in growth medium (high-glucose DMEM [Gibco 11965084]), supplemented with 10% fetal bovine serum (Sigma Aldrich F0926), and 1% penicillin/streptomycin (Gibco 15140122). Cells were grown to 80% to 90% confluence before medium was collected and replaced with serum-free RPMI medium (ThermoFisher 11875) for 24 hours before a collection of the serum-free medium was conducted. EVs were isolated by ultracentrifugation at 100 000 g for 70 minutes, then washed with sterile PBS and ultracentrifuged again at 100 000 g for another 70 minutes. The pellet was then resuspended in 10% dimethyl sulfoxide. A small aliquot was reserved for protein quantification, using a radioimmunoprecipitation assay (Pierce BCA Protein Assay Kit, ThermoFisher Scientific). A total of 50 µg of total protein was aliquoted and stored at –80°C in 10% dimethyl sulfoxide in PBS until usage. On the day of administration, protein was resuspended in 2 mL of 0.9% sterile saline.

EV Injection

Two weeks after ameroid placement, each of the ND and HFD groups were subdivided into 2 groups: controls (NDC: n=7; HFDC: n=6) and treatment groups (ND-EV: n=10; HFD-EV: n=8). All animals received the same operation where preoperative antibiotic regimen, anesthesia, and preparation were similar to the initial ameroid placement procedure. A small left thoracotomy incision was made 2 to 3 cm below the initial thoracotomy. The left atrioventricular groove was accessed and the ameroid constrictor visualized around the LCx. The ischemic territory was determined to be the area of the left ventricle within the distribution of the LCx. Intramyocardial injection of either 50 µg of EVs suspended in 2 mL of normal isotonic saline for the treatment subgroups (ND-EV and HFD-EV) or 2 mL of isotonic saline for the control subgroups (NDC and HFDC) was performed at 8 distinct sites throughout the ischemic area. Subsequently, the incision was closed in layers after careful hemostasis.

Terminal Harvest Procedure and Hemodynamic Measurements

Five weeks after the EV injection treatment, animals were euthanized in a terminal harvest procedure. Briefly, after induction of general anesthesia, femoral artery access was obtained and a pressure monitor catheter (Millar) was advanced in a retrograde fashion into the ascending aorta. The chest was entered through a median sternotomy. Five milliliters of Luteum and 5 mL of Europium-labeled microspheres were injected directly into the left atrium. During each injection, 10 mL of blood was drawn from the femoral catheter. This was repeated using 5 mL of Samarium-labeled microspheres with atrial pacing at 150 beats per minute. A 6F catheter sheath was introduced into the left ventricle through the apex, through which a pressure-volume monitoring catheter (Millar) was inserted. This allowed for recording of multiple hemodynamic parameters and plotting pressure volume loops under resting conditions, during atrial pacing at 150 beats per minute, and during occlusion of the inferior vena cava. Finally, after all measurements had been obtained, the animals were euthanized by means of exsanguination and heart excision. The ventricular tissue was quickly divided into 16 pieces and labeled according to the distribution of the LCx and left anterior descending coronary arteries. The tissue specimens were either placed in 10% formalin solution, flash frozen in liquid nitrogen, or air-dried for analysis of microsphere content. Proper care of animals was conducted as per the guidelines of the Principles of Laboratory Animal Care formulated by the National Society for Medical Research and the *Guide for the Care and Use of Laboratory Animals*.¹⁴

Metabolic Parameters

Before the terminal harvest procedures, whole blood samples were collected and sent to Rhode Island Hospital Central Laboratory for analysis. This included plasma levels of transaminases, bilirubin (total, direct), serum albumin, C-reactive protein, insulin, and a lipid profile.

Myocardial Perfusion

After the terminal procedure, left ventricular tissue within the distributions of the LCx and left anterior descending arteries were weighed, dried, and sent to Biophysics Assay Laboratory along with blood samples taken at various time points throughout both operations. Quantification of tissue microsphere content with respect to blood microsphere concentrations identified ischemic and nonischemic left ventricular territories and was used to calculate respective blood flow to the myocardial tissue segments.¹⁵

Immunofluorescence for Determination of Capillary and Arteriolar Density

Ischemic tissue specimens were fixed in 10% formalin for 24 hours before being transferred to 70% ethanol solution. The tissue was subsequently paraffinized and sectioned into 5- μ m slides, which were later deparaffinized and rehydrated through a series of washes from pure Xylene, to 100% EtOH, then 95% EtOH, 70% EtOH, 50% EtOH, and finally distilled H₂O. The slides were then stained for alpha smooth muscle actin (α SMA; Cell Signaling) and endothelial-marker CD31 (Abcam).

Slides were blocked in a peroxide solution, rinsed, and reblocked before being incubated in a 1:50 primary antibody solution overnight at 4°C. The next day, primary antibody solution was rinsed off, and a secondary antibody solution was added and incubated for 1 hour at room temperature. Last, the slides were mounted with Vectashield with DAPI (Vector Labs) and cover-slipped. Images were captured using a Nikon Eclipse TE2000-U microscope at 20 \times objective (Nikon Instruments). At least 3 images were captured per slide and analyzed using Image J software (National Institutes of Health) as previously described. Capillaries and arterioles were measured and counted using a 10-300 μ m particle and 300-infinity μ m particle analyzer tools, respectively.

Analysis of Protein Expression: Western Blotting

Flash-frozen tissue specimens collected from ischemic areas of the left ventricle were homogenized to make lysates. Concentration of protein was determined using a radioimmunoprecipitation assay (Pierce BCA Protein Assay Kit, Thermo Fisher Scientific). Whole-tissue lysates were fractionated onto 4% to 15% Tris-glycine Bio-Rad gels (Life Science Research) and transferred onto polyvinylidene fluoride membranes (Millipore). Blocking buffer (ThermoFisher Scientific) was applied for 1 hour before incubation with primary antibodies. Primary antibodies against endothelial nitric oxide synthase (eNOS), phosphorylated endothelial nitric oxide synthase, Akt (protein kinase B), phosphorylated Akt, MAPK ERK1/ERK2 (mitogen-activated protein kinase), phosphorylated MAPK, FOXO1 (forkhead box protein O1), phosphorylated FOXO1, TGF- β (transforming growth factor- β), VEGF (vascular endothelial growth factor) receptor 2 (VEGFR2), phosphorylated VEGFR2, BAX (BCL2-associated apoptosis regulator), and MMP-9 (matrix metalloproteinase 9), all from Cell Signaling, were applied at a 1:1000 dilution and incubated overnight at 4°C. Loading error was corrected using anti-GAPDH or anti- α -tubulin on all membranes. A secondary anti-rabbit antibody (Cell Signaling) was added at room

temperature for 1 hour. Images were visualized using a digital camera to capture enhanced chemiluminescence images (G-box, Syngene). Band densitometry was determined as arbitrary light units using Image-J software (National Institutes of Health). After normalization to GAPDH/ α -tubulin, data were obtained and presented as differences in mean and respective 95% CIs between groups.

Oxidative Stress: OxyBlot Protein Oxidation Detection Kit (S7150)

Oxyblot (Millipore) was performed on the ischemic and nonischemic myocardial tissue as per manufacturer protocol. Briefly, tissue was lysed in radioimmunoprecipitation assay buffer (Boston BioProducts) and 2 aliquots of each specimen were analyzed (1 aliquot was subjected to a derivatization reaction, while the other aliquot served as a negative control). A 5- μ L protein sample derived from each experimental animal was divided into 2 eppendorf tubes and then denatured with 12% sodium dodecyl sulfate. For the positive control, 2,4-dinitrophenylhydrazine solution was used to derivatize the samples. Derivatization control solution was used in the control samples. Both sets of samples were incubated at room temperature for 15 minutes after which neutralization solution was added. Finally, the 2 samples were loaded onto a polyacrylamide gel and followed by SDS-PAGE, Western blot transfer, and immunodetection.

Transcriptional Assay and mRNA Extraction: GeneChip Porcine Gene 1.0 ST Array

Ischemic ventricular myocardial tissue specimens were prepared (NDC, $n=3$; ND-EV, $n=3$; HFDC, $n=2$; HFD-EV, $n=3$) and carefully dissected free from the overlying epicardium while discarding endocardial remains to ensure that the sample was largely muscular in nature. Total RNA was isolated from this tissue by means of RNeasy Mini Kit (Qiagen). Subsequently, transcriptome profiling assay was performed with Applied Biosystems GeneChip Porcine Gene 1.0 ST Array (ThermoFisher Scientific) in accordance with the manufacturer's protocol at Brown University Genomics Core Facility using GeneChip 3000 instrument system. Gene expression array data were deposited to Gene Expression Omnibus (GEO) with accession number GSE154028.

Sample Size Justification

We previously determined the minimal sample size necessary to obtain statistically significant results to be 7 animals per group. This was done by analysis of previous protocols using a 2-tailed α level of 0.01, a B error level of 0.10, and the known SD of -0.15 .

Data Analysis

Gene Transcription Statistical Methods

From a total of 25 470 genes quantified, 7522 genes were successfully annotated. The arrays were then normalized and expression scores estimated by RMA (Irizarry et al, Biostatistics, 2003) and differential expression determined using the Limma R package (version 3.44.3) in R version 4.0.2. False discovery rate (FDR) q values were determined using the q value R package version 2.20.0. Genes with $q < 0.05$ were considered significant unless otherwise noted. Pathway enrichment was determined using ConsensusPathDB.

Of note, there were only 2 HFD animals not treated with EVs, and 3 animals in each of the other 3 groups. These analyses were exploratory with the intention of prioritizing next steps regarding gene transcription validation for future studies. Each gene was tested as a 2x2 factorial design in a Poisson generalized linear model (log link function used to parameterize as fold-differences). Classical sandwich estimation was used to adjust for any overdispersion/underdispersion. Each model had 7 effects estimated: main effects of diet and EV (2), interaction of EV and diet (1), and simple effects of diet and EV within effects of the levels of the other factor (4). For FDR, a total of 52 647 separate hypothesis tests from then factorial models (7×7521 genes) were subjected to an FDR adjustment. For inferences, following FDR adjustments, the adjusted interaction effects were examined. If the interaction effect adjusted P values were < 0.05 , then the main effects of the models were removed as oversimplifications. If the interaction-adjusted P values were not < 0.05 , then the simple effects were removed. This reduced the sample of relevant inferences to 22 695 adjusted P values.

Data were analyzed by means of a 2-way ANOVA test, with log-transformation of the dependent variable before analysis where appropriate. The main objective of these analyses was to elucidate any interaction between the effects of EV therapy and diet. In the absence of significant interaction, the main effects of each variable are reported. Last, multiple testing was corrected for using the Tukey method. All other data analyses were conducted using GraphPad Prism 7.04 (GraphPad Software Inc.) or SigmaPlot SYSTAT version 13.2 software (SYSTAT Software Inc), and are reported as mean and 95% CIs with respective P values for each group (NDC, ND-EV, HFDC, and HFD-EV).

RESULTS

Metabolic Parameters

The administration of HFD was associated with hypercholesterolemia as evidenced by elevated

total cholesterol and low-density lipoprotein levels. Although no significant change was observed in triglyceride levels, HFD was found to be associated with higher blood high-density lipoprotein levels. Fasting blood glucose concentration was higher in the HFD group, which, together with elevated blood fructosamine concentration, indicate that the HFD resulted in sustained hyperglycemia. Importantly, EV treatment resulted in a significant reduction in total cholesterol and low-density lipoprotein levels in HFD animals. The HFD group had higher basal serum concentrations of total bilirubin and alkaline phosphatase; however, EV administration was associated with a reduction in these markers of liver injury in both dietary groups. Finally, the HFD resulted in reduced concentrations of total protein and albumin, both of which were unaffected by EV treatment (Table).

Hemodynamic Measurements

HFD animals had higher heart rates (Figure 1D) and better preload-independent myocardial performance, ie, end-systolic pressure volume relationship at baseline (Figure 1B). EV therapy augmented cardiac output (Figure 1A), stroke volume (Figure 1C), and end-systolic pressure volume relationship (Figure 1B) in both dietary groups. The EV-treated myocardium showed significant improvement in relaxation and diastolic function, hence higher derivative of pressure over time (dp/dt min) (Figure 1E) and left ventricular diastolic time constant (Tau) (Figure 1F).

Myocardial Perfusion

EV treatment produced a significant increase in absolute blood flow in the ischemic myocardial tissue in both ND and HFD groups under resting conditions. Although no considerable difference was observed in myocardial blood flow between ND and HFD cohorts at baseline, the EV-induced increase in absolute blood flow was greater in the ND group. Neither diet nor EV treatment had any appreciable effect on perfusion during pacing at 150 beats per minute (Figure 2A and 2B).

Arteriolar and Capillary Density

Basal α SMA density quantified as percentage surface area was significantly higher in the ischemic myocardium of HFDC with respect to NDC animals. EV therapy was associated with a greater percentage increase in α SMA density in the ND than in the HFD animals (Figure 3A). We observed that increased CD31-labeled endothelial cell density in response to EV treatment in ND animals was absent in HFD tissue and did not reach statistical significance (Figure 3B).

Molecular Signaling: Protein Expression

Ischemic ventricular myocardium in both treated and control groups given an ND showed greater expression of total eNOS (Figure 4A), phosphorylated VEGFR2 (Figure 4D), FOXO1 (Figure 4E), phosphorylated MAPK ERK1/ERK2 (Figure 5B), and TGF- β

Table. Metabolic Parameters Assessed Between Groups by Means of 2-Way ANOVA

Metabolic Parameter	NDC	ND-EV	HFDC	HFD-EV	Effect of Diet <i>P</i> Value	Effect of EVs <i>P</i> Value
Glucose, mg/dL	102.42±5.54	101.33±4.51	128.00±5.45	133.00±5.79	0.0001	0.74
Fructosamine, μ MOL/L	194.43±5.44	194.4±1.84	229.33±11.13	216.13±9.57	0.0008	0.38
Cholesterol, mg/dL	64.71±3.11	58.90±3.48	973.50±118.5	476.88±60.87	0.0001	0.0002
LDL, mg/dL	25.14±2.02	23.80±2.054	867.17±119.77	377.88±58.94	0.0001	0.0002
HDL, mg/dL	35.86±1.71	31.50±2.35	102.50±5.16	93.88±5.96	0.0001	0.14
Triglycerides, mg/dL	18.57±2.79	18.50±2.64	18.50±2.45	25.50±2.26	0.22	0.22
ALT, U/L	56.43±2.21	44.40±2.97	45.83±4.81	33.50±1.31	0.0014	0.0004
AST, U/L	20.14±1.30	23.89±1.55	23.67±3.43	16.63±1.17	0.34	0.4
Alkaline phosphatase, IU/L	132.29±10.10	102.90±8.10	350.50±58.13	239.13±12.39	0.0001	0.0083
Bilirubin (total), mg/dL	0.10	0.10±0.06	0.22±0.02	0.14±0.02	0.0001	0.0007
Albumin, g/dL	2.33±0.08	2.18±0.06	2.02±0.07	2.11±0.05	0.0093	0.70
Total protein, g/dL	4.90	4.99±0.23	4.17±0.10	4.34±0.07	0.0001	0.39

High fat diet (HFD) produced significant hyperglycemia, hence elevated blood glucose levels at the time of terminal harvest procedures. High serum fructosamine concentrations further support that this hyperglycemic state was persistent over the course of the preceding weeks, which coincided with coronary stenosis following placement of the ameroid constrictor. A lipid panel shows that HFD was associated with hypercholesterolemia, high total cholesterol, and low-density lipoprotein (LDL) levels. Interestingly, extracellular vesicle (EV)-treated animals in the HFD group had significantly lower levels of cholesterol and LDL. HFD raised serum high-density lipoprotein (HDL) levels, whereas plasma triglyceride concentration was not significantly affected by this diet. We report reduced alanine aminotransferase (ALT) and aspartate aminotransferase (AST) levels in the HFD group when compared with those in the normal diet (ND) cohort. Conversely, HFD was associated higher alkaline phosphatase and total bilirubin levels whereas lower concentrations of serum albumin and total protein are seen in this dietary group. HFDC indicated high fat diet control; and NDC, normal diet control.

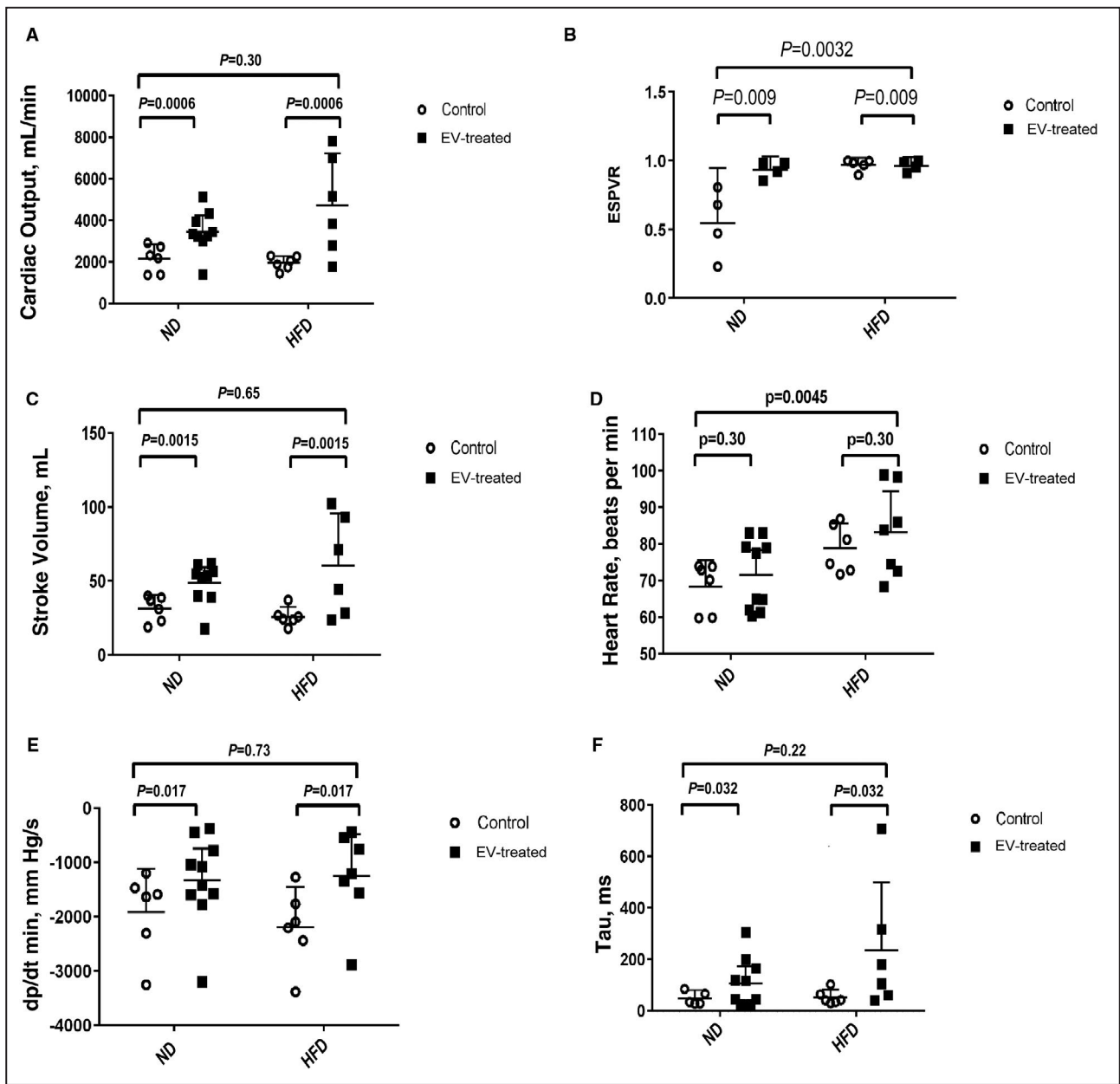


Figure 1. Analysis of hemodynamic parameters using 2-way ANOVA.

Higher baseline heart rate in the high fat diet (HFD) (D) is offset by greater preload-independent contractile performance, ie, end-systolic pressure volume relationship (ESPVR) (B). Extracellular vesicle (EV) therapy augmented (A) cardiac output, (B) ESPVR, and (C) stroke volume. The EV-treated myocardium showed enhanced ventricular relaxation, seen as a rise in (E) derivative pressure over time (dp/dt min) and improved diastolic performance denoted by increased (F) left ventricular diastolic time constant (Tau) in both the normal diet (ND) and HFD groups.

(Figure 5E) with respect to their HFD counterparts. Interestingly, ischemic ventricular tissue from HFD animals demonstrated appreciably higher levels of total VEGFR2 (Figure 4C), total MAPK ERK1/ERK2(Figure 5A), phosphorylated eNOS, and phosphorylated FOXO1 (Figure 4B and 4F) when compared with ND animals. There was no difference in the expression of total or phosphorylated Akt between the groups (Figure 5C and 5D). Quantification

of levels of BAX demonstrated a significant association between HFD and diminished expression of this proapoptotic protein (Figure 6A). Consistently, MMP-9 levels were reduced in the ischemic tissue lysates of HFD groups when compared with that from ND groups (Figure 6B). No observable effects could be attributed to EV therapy with respect to the expression of the aforementioned proteins in either group.

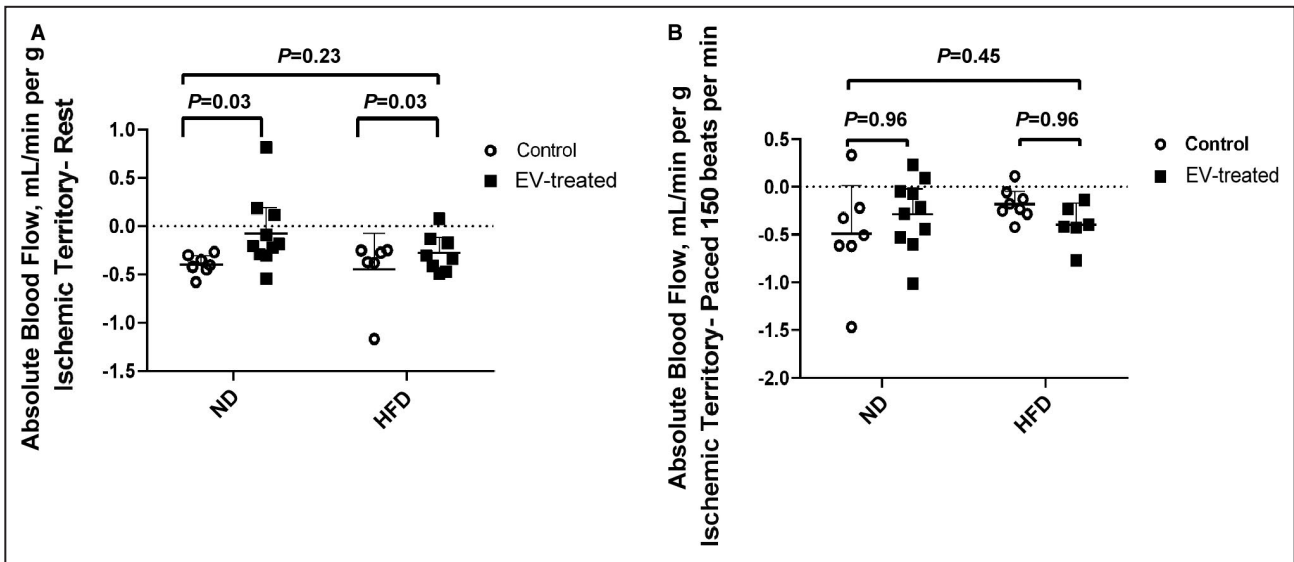


Figure 2. Measures of myocardial perfusion were compared between the 4 groups by means of 2-way ANOVA. Extracellular vesicle (EV) therapy was associated with significant increase in absolute blood flow to ischemic myocardial territories under resting conditions in both normal diet (ND) and high fat diet (HFD) groups (A). However, no appreciable difference in collateral-dependent perfusion was observable with EV therapy in either dietary cohort while pacing at 150 beats per minute (B).

Oxidative Stress: OxyBlot Analysis

Administration of EVs effectively ameliorated oxidative stress in both ND and HFD diet groups. Surprisingly, no appreciable difference was found at baseline between ND and HFD groups (Figure 6C), indicating that the expected burden of oxidative stress in HFD tissue was somehow mitigated.

Transcriptional Assay: mRNA Expression

Using an elegant 2x2 design, the effects of EV treatment versus no treatment depending on diet were

assessed with all hypothesis tests depicted in Table S1. First, the interaction, or the effect of EVs on the 2 diets, were determined to be statistically significant or insignificant for a set of genes (Figure 7A). Next, genes were separately examined according to significant and insignificant interaction, by the fold difference in expression between EV treatment and control in HFD and ND. Consistently, for the set of genes that did not show any interaction, ie, an effect of diet on EV treatment, the relative expression was more similar across diets (Figure B). Figure 7C,

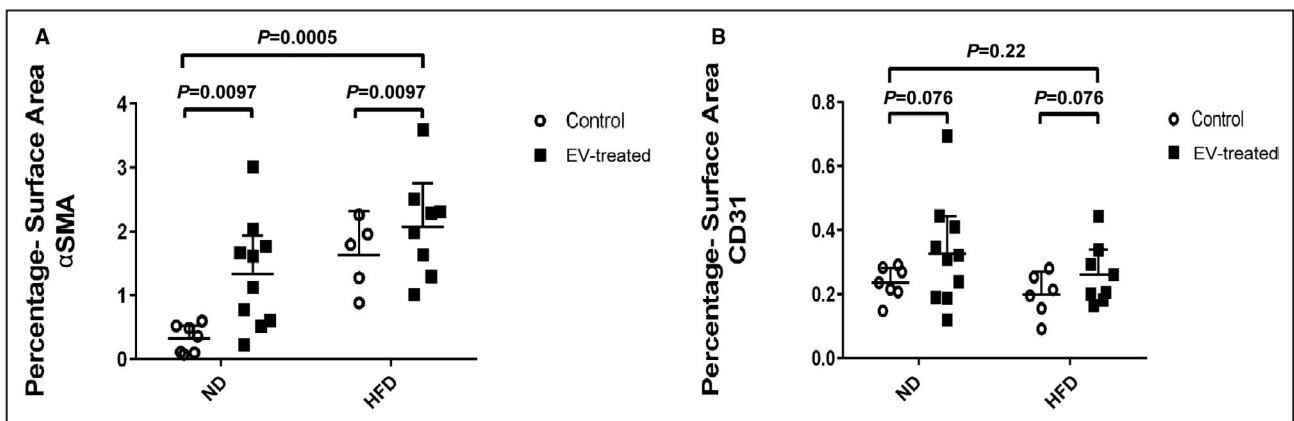


Figure 3. Vascular density was assessed by 2-way ANOVA. (A) Alpha smooth muscle actin (αSMA) density was higher at baseline in the high fat diet (HFD) ischemic myocardial territory when compared with that of the normal diet (ND) group. Extracellular vesicle (EV) therapy promoted arteriogenesis in both the HFD and ND groups. (B) Although a modest rise of CD31 endothelial density was seen with EV treatment in ischemic territories of the myocardium in ND animals, this did not reach statistical significance and was not recapitulated in the HFD group, indicating that the HFD was associated with inhibition of the angiogenic response to EVs. Images of αSMA and CD31 staining of ischemic myocardial sections can be found in previous publications relating to this project^{10,11} which are included in the supplementary material.

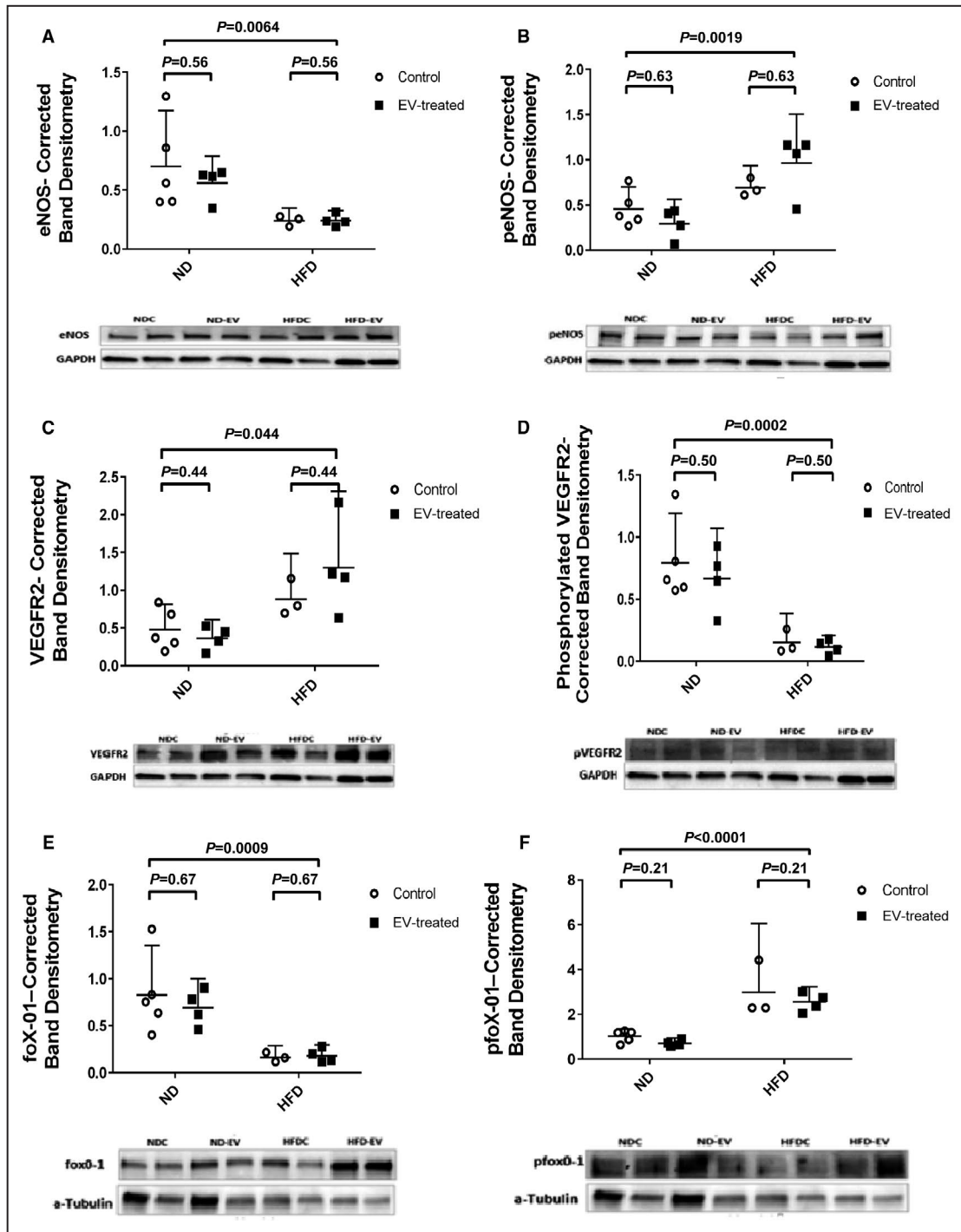


Figure 4. Comparing protein expression between groups by means of 2-way ANOVA. High fat diet (HFD) is associated with paradoxical molecular signaling including: (A) significantly lower levels of total endothelial nitric oxide synthase (eNOS) in the ischemic myocardium (B) but increased phosphorylation of this protein. Conversely, HFD seems to adversely affect phosphorylation of (D) VEGFR2 (vascular endothelial growth factor receptor 2) with a resultant greater pool of total (C) VEGFR2. Lower total levels of (E) FOXO1 (forkhead box protein O1) seen in HFD myocardial lysates correlate with a higher quantity of (F) phosphorylated protein. Data are presented diagrammatically, with corresponding images of selected representative gels from 3 consecutive experiments.

however, captures the changes in gene expression of EV treatment between HFD and ND for genes significantly affected by diet. Many genes upregulated in

ND were found to be less upregulated, even downregulated, or not regulated at all in HFD. Similarly, for genes downregulated in ND, these genes in HFD

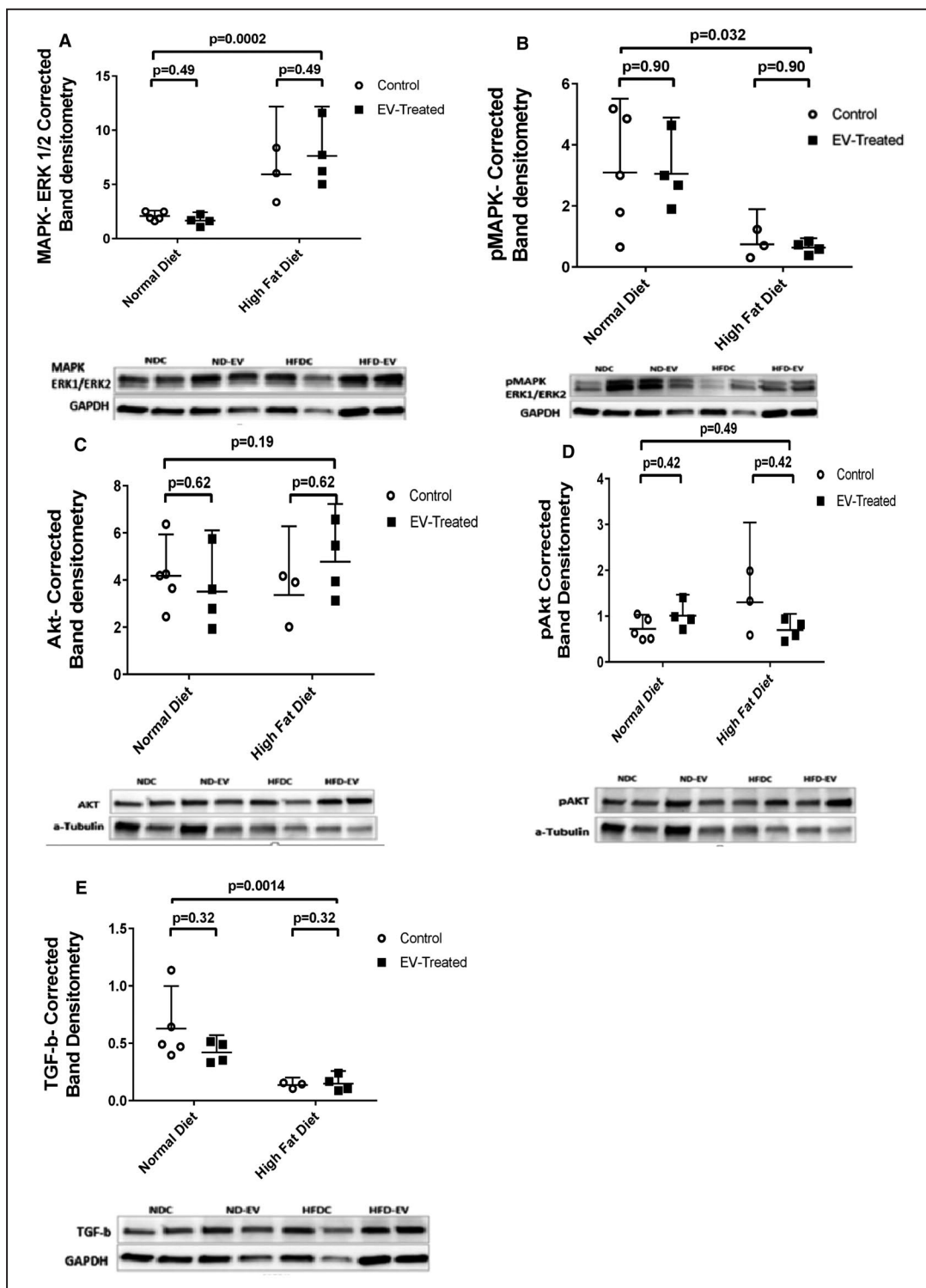


Figure 5. Paradoxical signaling cont'd.

Higher levels of (A) total MAPK ERK1/ERK2 (mitogen-activated protein kinase) are observed in ischemic myocardial lysates of high fat diet (HFD) animals but (B) phosphorylation of this protein is inhibited in this group. There is no observable change in the expression of (C) total Akt (protein kinase B) between the groups; however, (D) phosphorylated levels are significantly increased in the HFD group. Interestingly, the HFD is attributed to a reduction in the expression of (E) TGF-β (transforming growth factor-β), suggesting that alternative molecular signals may be implicated in the fibrotic response to metabolic stress.

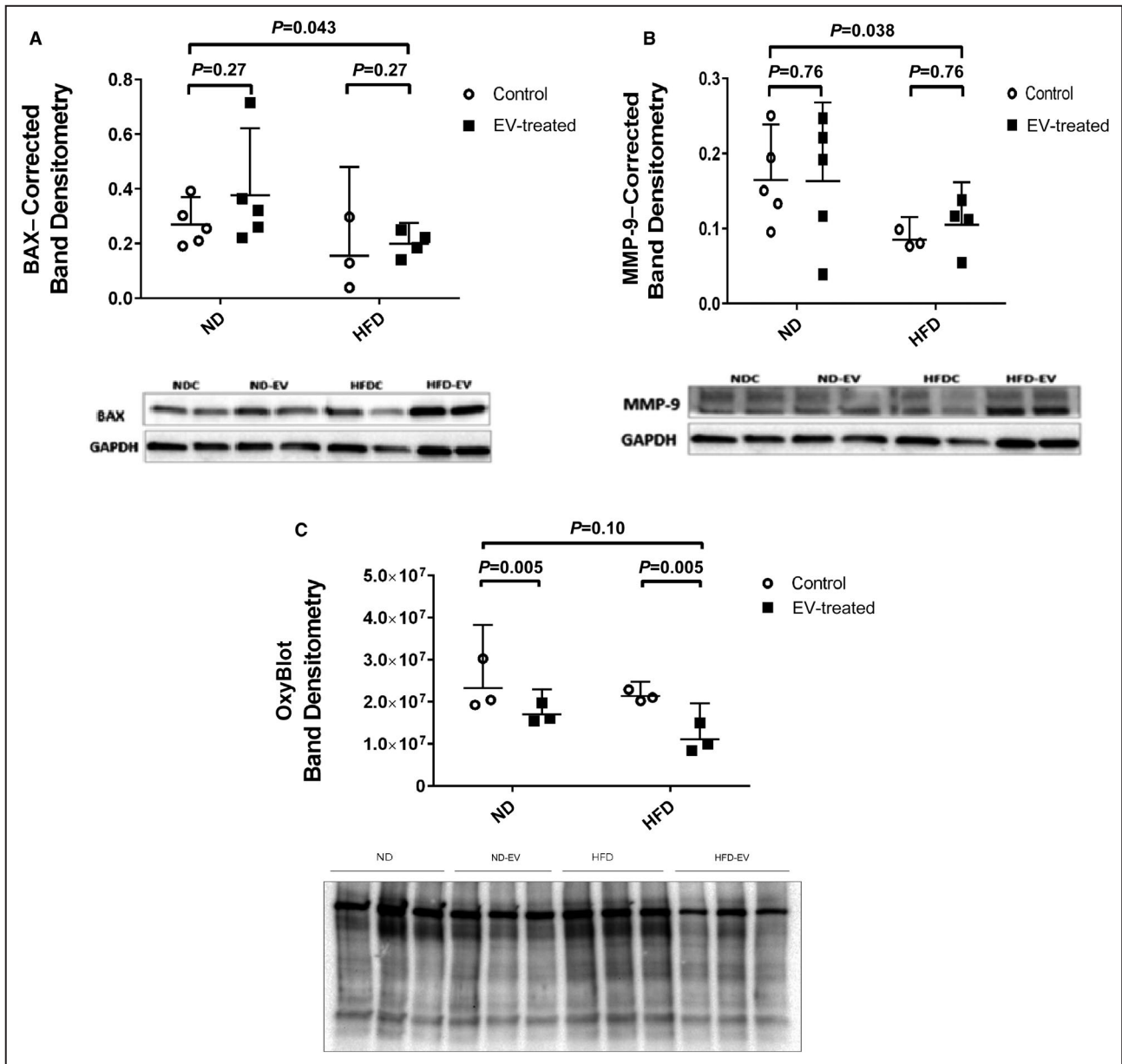


Figure 6. Concentrations of apoptotic proteins in myocardial lysates were studied among groups using 2-way ANOVA. High fat diet (HFD) inhibits the expression of the proapoptotic protein (A) BAX (BCL2-associated apoptosis regulator) and (B) MMP-9 (matrix metalloproteinase 9) in the ischemic myocardium. This may comprise an adaptive mechanism to promote survival in response to metabolic stress. (C) OxyBlot analysis showing a reduction of oxidative stress in the extracellular vesicle (EV)-treated myocardium in both normal diet (ND) and HFD groups. However, no significant difference in oxidative stress could be appreciated at baseline between the dietary groups.

were less downregulated, upregulated, or again not regulated. This contrasting pattern of gene expression, with few exceptions, highlights the disparate effects of EV therapy with respect to NDs and HFDs, and is consistent in heat map and pathway enrichment analyses (Figure 8A through 8E).

Heat map analysis of the relative expression between significant differentially expressed genes qualitatively displays that while EV treatment in ND altered gene expression, it had little effect (Figure 8A)

in HFD. The effect of diet (NDC and HFDC; Figure 8B) on gene expression is also apparent and reasonably appeared to associate with changes in metabolic processes, such as protein processing and oxidative phosphorylation, which is also reiterated when comparing the effect of EVs across diet (ND-EV and HFD-EV; Figure 8C). EV treatment alone in ND (ND-EV and NDC; Figure 8D) resulted in genes enriched in aerobic respiration—electron transport chain, oxidative phosphorylation, and complex I biogenesis;

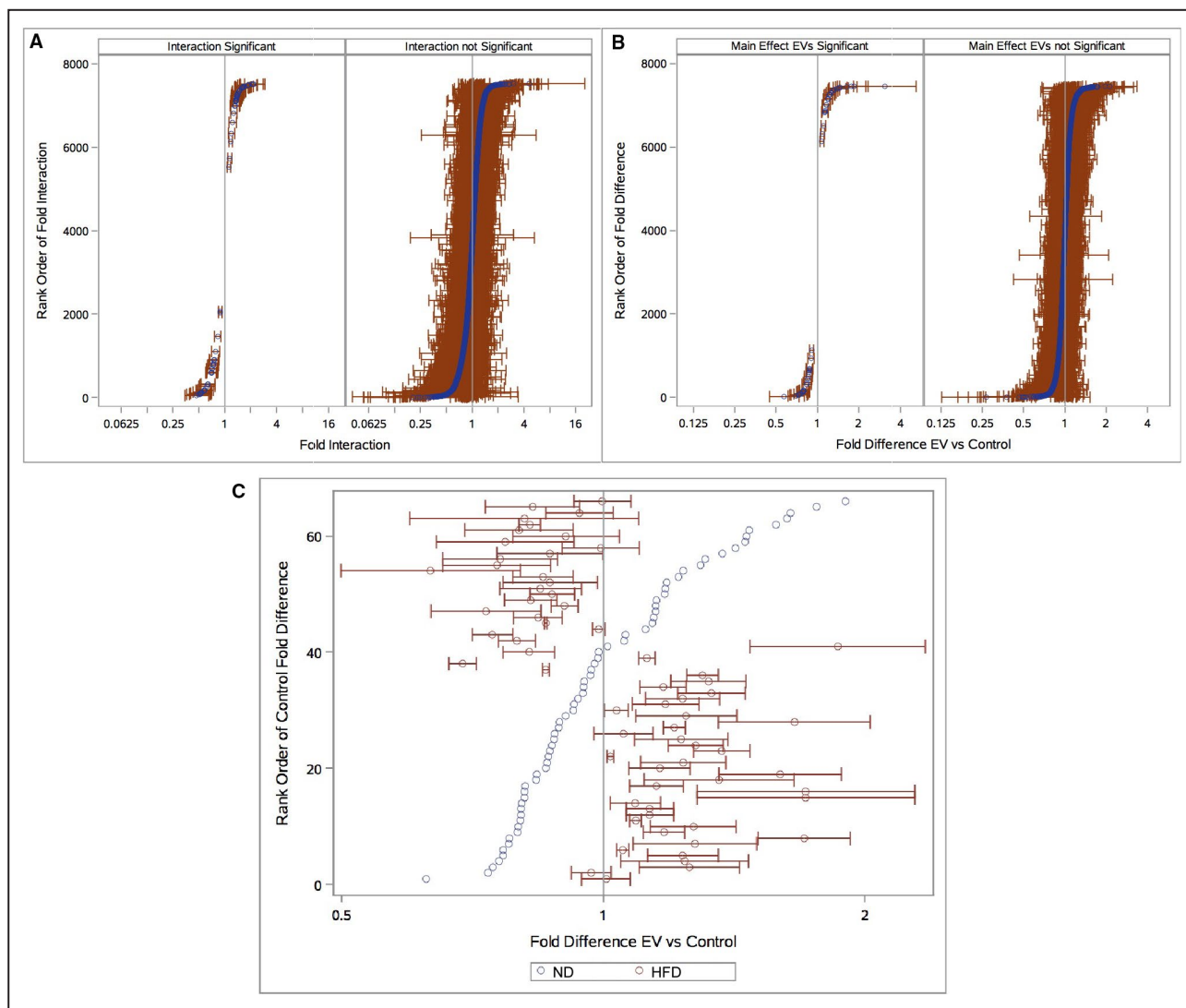


Figure 7. Relative effects of extracellular vesicles (EVs) on Diet.

(A) Rank-ordered by the magnitude of interaction from the most relative upregulation to downregulation with EV treatment in high fat diet (HFD) (red) vs normal diet (ND) (blue). Effects are depicted as significant or insignificant post–false discovery rate (FDR). (B) Fold difference in expression of EV treatment vs control in HFD and ND, for genes that did not show a significant interaction across diets. Again, statistically significant and insignificant genes after FDR are depicted. (C) Fold difference in expression of EV treatment vs control in HFD and ND, for genes with significant interaction between diets. FDR-adjusted *P* values of <0.05 were considered statistically significant, and HFD data points are depicted with 95% CIs.

whereas differentially expressed genes in EV treatment in HFD (HFD-EV and NDC; Figure 8E) were notably concentrated in pathways of immunity.

DISCUSSION

There is an emerging interest in EVs as a potential therapeutic modality for ischemic heart disease. We, among others, have shown the beneficial effects of such therapy in chronic myocardial ischemia, ie, improved collateral-dependent perfusion and vessel formation with a greater degree of preservation of contractile function. In

this regard, EVs are an excellent example of a prospective treatment; however, this study importantly indicates that a favorable tissue response is diminished by metabolic dysregulation that occurs with hyperglycemia and dyslipidemia. Indeed, EV augmentation of myocardial blood flow and vascular density in the ischemic myocardium was inhibited by the HFD. We further report a number of alterations that reflect a profound disruption of the molecular niche and are consistent with cellular stress in the HFD group.

A main objective of this study was to elucidate aberrant signaling mechanisms that contribute to impaired angiogenesis seen with hyperglycemia and

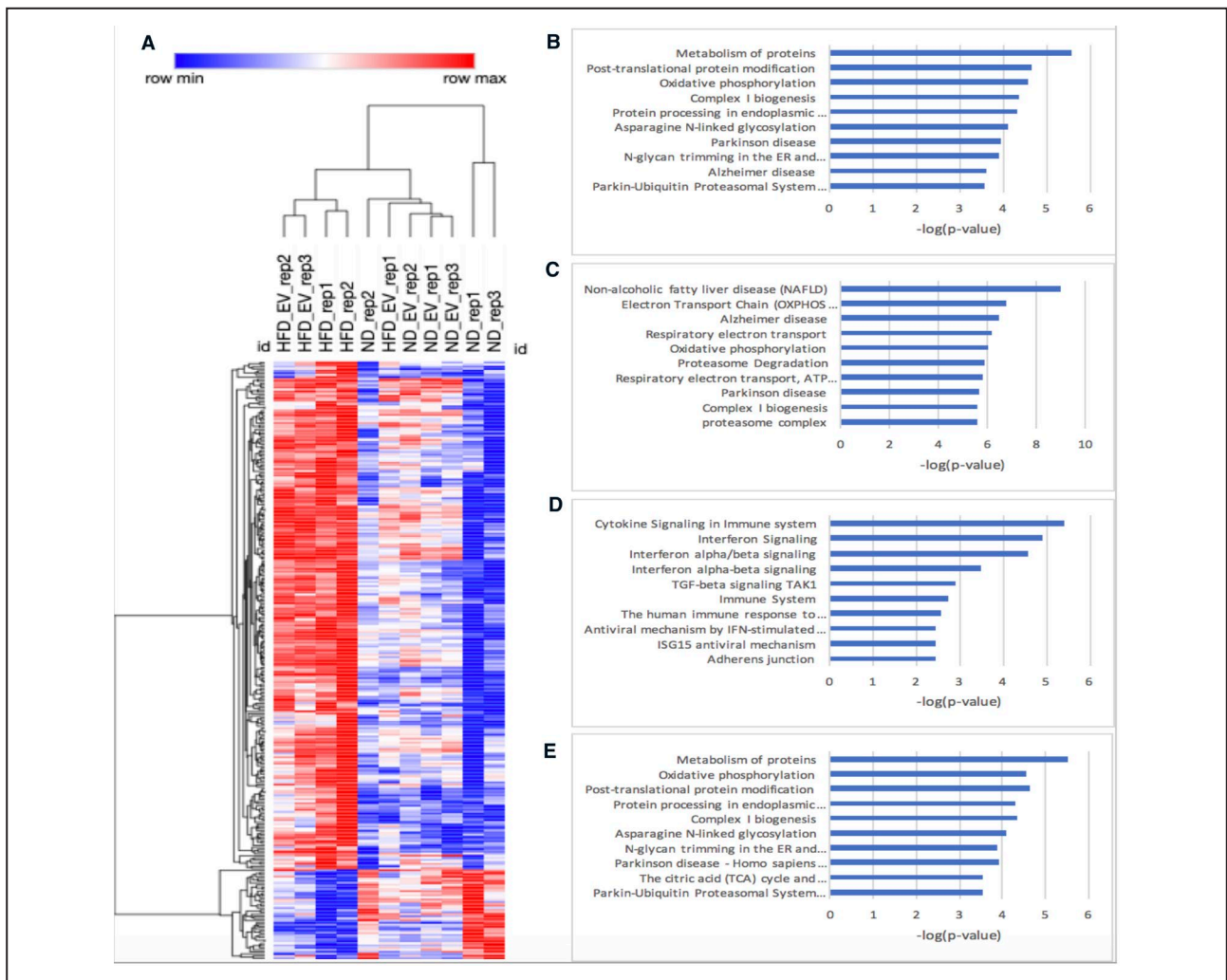


Figure 8. Relative gene expression and pathway analysis.

(A) Heat map analysis of relative expression in replicates within each group, for significant genes ($q < 0.05$) identified in the normal diet (ND) extracellular vesicle (EV)-treated (ND-EV) vs high fat diet EV (HFD-EV)-treated comparison. Pathway enrichment analysis (<http://cpdb.molgen.mpg.de/>) was performed with significantly differentially expressed genes ($q < 0.05$) between the following comparisons: (B) ND control (NDC) and HFD control (HFDC), (C) ND-EV and NDC*, (D) HFD-EV and HFDC*, and (E) ND-EV and HFD-EV. *Note inclusion criteria for differentially expressed genes in these comparisons were $P < 0.05$, in place of $q < 0.05$.

dyslipidemia. Despite gross blood flow data showing enhanced collateral-dependent perfusion to the ischemic myocardium with EVs in both dietary groups, the response in the HFD group was diminished. Interestingly, a higher level of arteriolar (α SMA) density is seen in the high fat group at baseline, which was unmatched by a corresponding rise in CD31 endothelial cell density. In the interpretation of these results, we recognize that the vascular response observed in the ischemic myocardium in our model is consistent with adaptive arteriogenesis, a term often used interchangeably with collateralization. However, arteriogenesis is a distinct process that is initiated by the inflammatory response-directed growth of vascular smooth muscle cells and their migration in an epicardial to endocardial direction. Perhaps an

HFD-imposed inflammatory state explains the finding of higher α SMA density in this group. Subsequently, flow-dependent endothelial cell homing and proliferation must occur before remodeling in order to complete the formation of competent vasculature.¹⁶ Endothelial viability is key, and maintenance of the nascent endothelium requires an intact growth factor-response mechanism. Our findings indicate that the HFD results in dysregulation of a number of processes vital to the VEGFR2 signaling mechanism. More specifically, we identified deficient phosphorylation of the VEGFR2 in the HFD tissue. Upregulation of downstream elements, hence increased phosphorylation of eNOS and FOXO1, may conceivably be a compensatory response that serves to salvage endothelial reserve and restore euglycemic state.¹⁷

Interestingly, we report a reduction in the expression of TGF- β and MMP-9 in HFD ischemic myocardial lysates. Although conventionally used as markers for fibrosis and apoptosis, TGF- β and MMP-9 signaling have important roles in supporting angiogenesis by remodeling basement membranes, releasing VEGF from matrix stores and potentiating VEGF-dependent endothelial migration and proliferation.^{18,19}

These data underscore the negative effect of HFD on myocardial collateral blood flow to ischemic myocardium, albeit accentuated vascular myogenesis. Alternatively, ND endothelial tissue shows a capacity to form collateral vessels when treated with EVs. This is evident by endothelial cell proliferation that is supported by protein expression consistent with angiogenic activity. Importantly, this study identifies molecular anomalies that may diminish the efficacy of therapeutic angiogenesis in the setting of hyperglycemia or dyslipidemia.

An analysis of myocardial hemodynamic performance shows that EV therapy positively affected stroke volume, cardiac output, and the end-systolic pressure volume relationship in both dietary cohorts. These data, taken together with our findings of improved measures of myocardial relaxation in EV treatment cohorts, eg, Tau and dp/dt min, indicate that EVs improved preload-independent contractility (end-systolic pressure volume relationship) while potentially ameliorating diastolic dysfunction in the ischemic myocardium. Notably, we found greater preload-independent myocardial contractile performance in HFD animals at baseline. This may have offset compromised filling time seen at higher heart rates in this group, to produce the lack of difference in stroke volume when compared with ND counterparts.

Although beyond the scope of this study, we found that EV treatment was associated with a significant reduction in serum cholesterol and low-density lipoprotein levels in the HFD group. This remarkable finding indicates that despite the low dose administered locally to the ventricular myocardium, EVs were able to positively modulate hepatic cholesterol regulation.

Apoptosis is known to complicate myocardial ischemia and contributes to deterioration in myocardial function. We show that cells respond to metabolic stress in HFD by negatively regulating apoptotic mechanisms. Among the paradoxical molecular signaling elucidated in HFD tissue, reduced phosphorylation of MAPK ERK1/ERK2 may aim to inhibit ERK1/2-mediated apoptotic pathways.²⁰ Consistently, HFD is associated with reduced expression of the proapoptotic protein BAX.

EV therapy effectively reduced oxidative stress in the ischemic myocardium of both dietary cohorts. We did not find a significant difference in oxidative stress between the NDC and HFDC groups at baseline. This may in part be caused by heightened functioning

antioxidant mechanisms in an effort to neutralize reactive oxidative species with dyslipidemia and diabetes mellitus.

FUTURE DIRECTIONS

In this study, we identified a number of metabolically dysregulated molecular and genetic targets that undermine the ability of the ischemic myocardium in HFD animals to revascularize in response to a novel therapeutic agent. These findings were supported by clinically relevant gross parameters such as myocardial perfusion, coronary collateral formation, and myocardial functional performance in a validated translational model.

Our work confirms that adaptive arteriogenesis is the predominant response of the ischemic myocardium aimed at restoring blood flow. Furthermore, we show that HFD induced greater inflammation-mediated recruitment of vascular smooth muscle cells. However, endothelial migration, proliferation, and survival were paradoxically inhibited in this group. The VEGF-VEGFR2 signaling mechanism is key to endothelial function, and defects in this mechanism are largely implicated in a hindered angiogenic capacity.²¹ To date, the exact mechanisms by which metabolic disorders such as hyperglycemia and dyslipidemia contribute to VEGF dysfunction remain elusive.

Finally, EVs are versatile vehicles that enclose a multitude of signals including siRNA, transcription, and growth factors, and are capable of modifying a wide spectrum of processes ranging from epigenetic regulation to receptor mechanisms. One must be reminded that molecular aberrancies behave similarly to the disease processes they produce, seldom occurring in isolation. Therefore, an excellent therapeutic agent would be capable of targeted correction of multiple erroneous mechanisms in a coordinated manner. It is plausible that EVs could potentially be a milestone in revolutionizing molecular medicine. Further insight into the structure and composition of EVs would allow for structured incorporation of corrective signals that serve many applications including promoting angiogenesis to the chronically ischemic myocardium.

LIMITATIONS

This study is a continuum to our previous work.^{10,11} Animal tissue from experiments conducted and reported by our group was used for the applications listed above, conferring the limitations of that work to the study at hand. Certainly, the ability to study gross ventricular morphological characteristics would have yielded valuable data. Unfortunately, imaging

modalities such as echocardiography and/or magnetic resonance imaging were technically unfeasible, and perfusion study protocols mandated immediate sectioning and weighing of ventricular samples corresponding to vascular territories, which precluded postmortem studies of gross pathology.

It is reasonable to believe that the 5-week interval between EV administration and the terminal harvest procedure falls short of the duration that defines this disease process in humans and that this limited time-frame may well have contributed to underestimation of the efficacy of EVs to develop vascular networks. We will be reevaluating this timeline considering species-specific growth patterns among other factors. Similarly, the dose of EVs effectively delivered to the myocardium was relatively low when considering the large size of the animals' hearts. The method of administration of EVs used in our swine model was unconventional with virtually no dosing recommendations available in the literature. This led us to use an arbitrary-trial dose for our experiments. However, the prospective use of a cost-effective small animal model would allow for studying dose-response characteristics.

Another limitation is our exclusive use of intact male swine, which we believe confers the added risk of coronary heart disease in the male population.²² Nevertheless, we will be including female animals in future experiments and it would be interesting to observe for sex-specific differences. We did not achieve a complete metabolic profile in the HFD group consistent with the metabolic syndrome in humans; however, we show that this diet resulted in profound hypercholesterolemia and hyperglycemia in our swine model, which produced significant metabolic derangement. Importantly, we have unraveled a prospective basis for a hypothesis as to the mechanisms by which EVs exert their effects.

It is important to note that one round of quantitative reverse transcription polymerase chain reaction was performed with genes of interest and those randomly selected. A few genes had inconsistent results to the transcriptomics microarray, whereas functional primers could not be obtained for others. We plan to perform additional trials in the future to increase sample number; our current ability to conduct additional trials is limited by the coronavirus disease 2019 (COVID-19) pandemic.

Regarding the gene expression statistical analysis, there were conservative choices made for this approach: (1) classically, the 3 omnibus effects (2 main effects and 1 interaction) are not adjusted for multiplicity, and (2) the interaction effect is often used as a gatekeeper for whether to calculate simple effects. Therefore, including all 7 effects per gene in the FDR adjustments would be considered relatively conservative. Another conservative aspect of the approach is in not accommodating correlated effects among correlated genes. At the same time, FDR methods

do *not* control type I error, making them generally more liberal. On balance, especially when considering our limited sample size, we consider these analyses as fair but in need of replication with larger sample sizes as next steps. Therefore, our future gene expression study will comprise larger sample size, further substantiation by quantitative reverse transcription polymerase chain reaction, and elucidation of intracellular signaling mechanisms, in accordance with protein expression data through immunoblotting and/or proteomics.

CONCLUSIONS

Overall, the larger picture remains obscure and much work will be needed to determine the contents of these vesicles under various conditions and how this can be altered to incorporate target signaling molecules. Accordingly, the pharmacodynamic properties of EVs are yet to be characterized. This insight may also allow for refinement of their route of administration. Ongoing studies by our group will address these questions in the future.

ARTICLE INFORMATION

Received May 8, 2020; accepted October 12, 2020.

Affiliations

From the Division of Cardiothoracic Surgery, Alpert Medical School of Brown University and Rhode Island Hospital, Providence, RI (A.A., B.A.P., L.A.S., C.K., G.S., Z.Z., K.B., M.P., N.R.S., M.R.A., F.W.S.); Department of Surgery (A.A., B.A.P., L.A.S., Z.Z., J.T.M., N.R.S., M.R.A., F.W.S.) and Department of Orthopedics (J.T.M.), Alpert Medical School of Brown University, Providence, RI; Biostatistics Core, Lifespan Hospital System, Providence, RI (J.T.M.); Department of Molecular Biology, Cell Biology, Biochemistry, Genomics Core, Brown University, Providence, RI (C.S.); Department of Pathology and Laboratory Medicine, Alpert Medical School of Brown University, Providence, RI (A.S.B.); Center for Computational Molecular Biology, Brown University, Providence, RI (A.S.B.); and Cardiothoracic Surgery Division, Cardiovascular Research Center, Rhode Island Hospital, Warren Alpert Medical School of Brown University, Providence, RI (M.G., O.C.).

Acknowledgments

The authors thank Dr Richard Clements; Tiffany M. Borjeson, DVM; Jessica Johnston, DVM; Jessica Fernandes; Cindy Phun; Maria Veliz; and Virginia Hovanesian.

Sources of Funding

Funding for this research was provided by the National Heart, Lung, and Blood Institute (NHLBI) (R01HL46716, R01HL128831-01A1, and P20 GM103652 to F.W.S.); NHLBI (1R01HL133624 to M.R.A.); National Institutes of Health/National Institute of General Medical Sciences training grant (2T32 GM065085 to B.A.P. and L.A.S.).

Disclosures

None.

Supplementary Material

Table S1

REFERENCES

1. Nowbar AN, Gitto M, Howard JP, Francis DP, Al-Lamee R. Mortality from ischemic heart disease: analysis of data from the world health organization and coronary artery disease risk factors from NCD risk factor

- collaboration. *Circulation Cardiovasc Qual Outcomes*. 2019;12:e005375. DOI: 10.1161/CIRCOUTCOMES.118.005375.
2. Fihn SD, Gardin JM, Abrams J, Berra K, Blankenship JC, Dallas AP, Douglas PS, Foody JM, Gerber TC, Hinderliter AL, et al. 2012 ACCF/AHA/ACP/AATS/PCNA/SCAI/STS guideline for the diagnosis and management of patients with stable ischemic heart disease. *J Am Coll Cardiol*. 2012;60:e44–e164.
 3. Levine GN, Bates ER, Blankenship JC, Bailey SR, Bittl JA, Cercek B, Chambers CE, Ellis SG, Guyton RA, Hollenberg SM, et al. ACCF/AHA/SCAI guideline for percutaneous coronary intervention. *J Am Coll Cardiol*. 2011;58:e123–e210.
 4. Hillis LD, Smith PK, Anderson JL, Bittl JA, Bridges CR, Byrne JG, Cigarroa JE, DiSesa VJ, Hiratzka LF, Hutter AM, et al. ACCF/AHA guideline for coronary artery bypass graft surgery. *J Am Coll Cardiol*. 2011;58:e123–e210.
 5. Molgat AS, Tilokey EL, Rafatian G, Vulesevic B, Ruel M, Milne R, Suuronen EJDD. Hyperglycemia inhibits cardiac stem cell-mediated cardiac repair and angiogenic capacity. *Circulation*. 2014;130:S70–S76.
 6. Jang JJ, Ho HK, Kwan HH, Fajardo LF. Angiogenesis is impaired by hypercholesterolemia: role of asymmetric dimethylarginine. *Circulation*. 2000;102:1414–1419.
 7. Smith RR, Marbán E, Marbán L. Enhancing retention and efficacy of cardiosphere-derived cells administered after myocardial infarction using a hyaluronan-gelatin hydrogel. *Biomatter*. 2013;3:e24490.
 8. Grimaldi V, Mancini FP, Casamassimi A, Al-Omran M, Zullo A, Infante T, Napoli C. Potential benefits of cell therapy in coronary heart disease. *J Cardiol*. 2013;62:267–276.
 9. Andaloussi EL, Mäger I, Breakefield XO. Extracellular vesicles: biology and emerging therapeutic opportunities. *Nat Rev Drug Discov*. 2013;12:347–357.
 10. Potz BA, Scrimgeour LA, Pavlov VI, Sodha NR, Ruhul Abid MS, Sellke FW. Extracellular vesicle injection improves myocardial function and increases angiogenesis in a swine model of chronic ischemia. *J Am Heart Assoc*. 2018;7:e008344. DOI: 10.1161/JAHA.117.008344.
 11. Scrimgeour LA, Potz BA, Aboul Gheit A, Shi G, Stanley M, Zhang Z, Ahsan NA, Ruhul Abid MS, Sellke FW. Extracellular vesicles promote arteriogenesis in chronically ischemic myocardium in the setting of metabolic syndrome. *J Am Heart Assoc*. 2019;8:e012617. DOI: 10.1161/JAHA.119.012617.
 12. Lerman XZ. Investigating the metabolic syndrome: contributions of swine models. *Toxicol Pathol*. 2016;44:358.
 13. Radke PW, Heintz-Green A, Frass OM, Post MJ, Sato K, Geddes DM. Evaluation of the porcine ameroid constrictor model of myocardial ischemia for therapeutic angiogenesis studies. *Endothelium*. 2006;13:25–33.
 14. Council NR. Guide for the Care and Use of Laboratory Animals. 2011.
 15. Schuster A, Sinclair M, Zarinabad N, Ishida M, Van Den Wijngaard JP, Paul M, Van Horssen P, Hussain ST, Perera D, Schaeffter T, et al. A quantitative high resolution voxel-wise assessment of myocardial blood flow from contrast-enhanced first-pass magnetic resonance perfusion imaging: microsphere validation in a magnetic resonance compatible free beating explanted pig heart model. *Eur Heart J Cardiovasc Imaging*. 2015;16:1082–1092.
 16. Conway EM, Collen D, Carmeliet P. Molecular mechanisms of blood vessel growth. *Cardiovasc Res*. 2001;49:507–521.
 17. Dominy JE, Puigserver P. Nuclear FoxO1 inflames insulin resistance. *EMBO J*. 2010;29:4068–4069.
 18. Carmeliet P, Jain RK. Molecular mechanisms and clinical applications of angiogenesis. *Nature*. 2011;473:298–307.
 19. Goumans MJ, Valdimarsdottir G, Itoh S, Rosendahl A, Pideras S, ten Dijke P. Balancing the activation state of the endothelium via two distinct TGF- β type I receptors. *EMBO J*. 2002;21:1743–1753.
 20. Mebratu Y, Tesfayiz Y. How ERK1/2 activation controls cell proliferation and cell death is subcellular localization the answer? *Cell Cycle*. 2009;8:1168–1175.
 21. Claesson-Welsh L. Signal transduction by vascular endothelial growth factor receptors. *Biochem Soc Trans*. 2003;31:20–24.
 22. Jousilahti P, Vartiainen E, Tuomilehto J, Puska P. Sex, age, cardiovascular risk factors, and coronary heart disease a prospective follow-up study of 14 786 middle-aged men and women in Finland. *Circulation*. 1999;99:1165–1172.

SUPPLEMENTAL MATERIAL

The FREQ Procedure

Frequency

Table of Interpretation by Label								
Interpretation	Label							
	Difference in Effects	Main Effect HFD	Main Effect MVs	Simple Effect of High Fat Diet with MVs	Simple Effect of High Fat Diet without MVs	Simple Effect of MVs in High Fat Diet	Simple Effect of MVs in Normal Diet	Total
Diet did not significantly regulate gene with MVs	0	0	0	54	0	0	0	54
Diet did not significantly regulate gene without MVs	0	0	0	0	24	0	0	24
Diet did not significantly regulate gene, regardless of MVs	0	7089	0	0	0	0	0	7089
Gene more downregulated or less upregulated by MVs in High Fat diet than Normal (see Simple effects)	28	0	0	0	0	0	0	28
Gene more upregulated or less downregulated by MVs in High Fat diet than Normal (see Simple effects)	38	0	0	0	0	0	0	38
High Fat Diet downregulated gene relative to Normal Diet similarly, regardless of MVs	0	84	0	0	0	0	0	84
High Fat Diet downregulated gene relative to Normal Diet with MVs	0	0	0	3	0	0	0	3
High Fat Diet downregulated gene relative to Normal Diet without MVs	0	0	0	0	21	0	0	21
High Fat Diet upregulated gene relative to Normal Diet similarly, regardless of MVs	0	282	0	0	0	0	0	282
High Fat Diet upregulated gene relative to Normal Diet with MVs	0	0	0	9	0	0	0	9
High Fat Diet upregulated gene relative to Normal Diet without MVs	0	0	0	0	21	0	0	21
MVs did not significantly regulate gene with High Fat Diet	0	0	0	0	0	37	0	37
MVs did not significantly regulate gene with Normal Diet	0	0	0	0	0	0	47	47
MVs did not significantly regulate gene, regardless of Diet	0	0	7412	0	0	0	0	7412
MVs downregulated gene relative to vehicle alone similarly, regardless of Diet	0	0	21	0	0	0	0	21
MVs downregulated gene relative to vehicle alone with High Fat Diet	0	0	0	0	0	12	0	12
MVs downregulated gene relative to vehicle alone with Normal Diet	0	0	0	0	0	0	10	10
MVs upregulated gene relative to vehicle alone similarly, regardless of Diet	0	0	22	0	0	0	0	22
MVs upregulated gene relative to vehicle alone with High Fat Diet	0	0	0	0	0	17	0	17
MVs upregulated gene relative to vehicle alone with Normal Diet	0	0	0	0	0	0	9	9
The effect of MVs did not depend on diet or vice versa (look to Main Effects)	7455	0	0	0	0	0	0	7455
Total	7521	7455	7455	66	66	66	66	22695